frontiers | Frontiers in Earth Science

TYPE Original Research
PUBLISHED 23 January 2023
DOI 10.3389/feart.2023.1099178

Check for updates

OPEN ACCESS

EDITED BY
Nicola Colombo,
National Research Council (CNR), Italy

REVIEWED BY
Guitao Shi,
East China Normal University, China
Li Ming,
Jilin Jianzhu University, China
Jianzhong Xu,
Northwest Institute of Eco-Environment and Resources (CAS), China

*CORRESPONDENCE
Ninglian Wang,
nlwang@nwu.edu.cn

SPECIALTY SECTION
This article was submitted to Cryospheric Sciences, a section of the journal Frontiers in Earth Science

RECEIVED 15 November 2022
ACCEPTED 10 January 2023
PUBLISHED 23 January 2023

CITATION
Zhang Y, Wang N, Zhang B, Zhang W and Shen B (2023), Interannual variation and chemical characterization of major water-soluble inorganic ions in snow across Northwest China.
Front. Earth Sci. 11:1099178.
doi: 10.3389/feart.2023.1099178

Interannual variation and chemical characterization of major water-soluble inorganic ions in snow across Northwest China

Yuxuan Zhang[1,2], Ninglian Wang[1,2,3,4]*, Bo Zhang[1,2], Wei Zhang[1,2] and Baoshou Shen[1,2]

[1]Shaanxi Key Laboratory of Earth Surface System and Environmental Carrying Capacity, Northwest University, Xi'an, China, [2]College of Urban and Environmental Sciences, Northwest University, Xi'an, China, [3]Institute of Earth Surface System and Hazards, Northwest University, Xi'an, China, [4]Institute of Tibet Plateau Research, Chinese Academy of Sciences, Beijing, China

From November 2018 to April 2020, 438 snow samples were collected near two field observation sites in Heihe and Altay, Northwest China, and the pH and major water-soluble inorganic ions (Ca^{2+}, SO_4^{2-}, Na^+, NO_3^-, Cl^-, K^+, Mg^{2+}, and NH_4^+) were analyzed. To identify the source of ions, the enrichment factor method, Pearson correlation analysis, and HYSPLIT (Hybrid Single Practical Lagrangian Integrated Trajectory) backward trajectory analysis were employed. The snow was nearly pH neutral, and Ca^{2+} was the dominant cation present. The anion concentration demonstrated high variability. Affected by geographical location and atmospheric circulation, the concentration of soluble inorganic ions in snow from the Altay region was higher than that in the Heihe region and remote areas at high altitude or high latitude. Compared with 2018/2019, ion concentrations in snow increased in 2019/2020, especially in the Altay region. Moreover, the temporal trend of ion concentrations was stable, indicating that the source and migration path of ions had strong consistency. Our study suggested that terrestrial sources are the main driving factors for the ions observed in snow samples from Northwest China, and some ions are also the result of anthropogenic sources (NH_4^+, SO_4^{2-}, and NO_3^-), marine sources (Cl^- and Na^+), and salt mine dust (Cl^-, Na^+, SO_4^{2-}, and K^+).

KEYWORDS

water-soluble inorganic ions, Northwest China, snow, interannual variation, HYSPLIT (hybrid single-particle lagrangian integrated trajectory)

1 Introduction

Snow is an important wet deposition, especially at high altitudes and latitudes, that removes natural substances (e.g., sea salt and soil dust) and anthropogenic pollutants from the atmosphere (Sakihama et al., 2008; Steinhauser et al., 2008). Cold and dry in winter, snowpack is a good archive for atmospheric environment, among which water-soluble inorganic ions (mainly including Ca^{2+}, SO_4^{2-}, Na^+, NO_3^-, Cl^-, K^+, Mg^{2+}, and NH_4^+) are important indicators of climate change (Fuhrer et al., 1996; Olivier et al., 2006). In arid areas, snowmelt water is the main source of irrigation water and domestic water, and its quality and quantity are closely related to local residential domestic water and agricultural production (Null et al., 2010; Zhu, et al., 2018). Therefore, understanding the source and transport of major water-soluble inorganic ions in snow cover is important for understanding hydrological processes and vegetation growth (Thompson et al., 2000; Jeong and Sushama, 2018).

Snow cover is widely distributed in China, and the area of stable snow cover is about 4.2 million km^2 (Liand Mi, 1983). Snow cover in Northwest China is mainly distributed in northern Xinjiang and the northern edge of the Tibetan Plateau (Qin et al., 2006; Ma et al., 2018). A large number of studies have analyzed the chemical characteristics of snow and ice in China (Cui et al., 2014; Pu et al., 2017; Zhou et al., 2019). In Northeast China, Xue et al. (2020) found that ion concentrations reached their peak in the middle or later period of the snow season. In Northwest China, based on an analysis of snow pit samples of several glaciers (e.g., Tianshan No. 1 Glacier, Yushugou No. 6 Glacier, and Laohugou No. 12 Glacier), it was found that the main ions in snow were mainly from terrestrial dust (Xiao et al., 2008; Li et al., 2005; Li et al., 2010; Liu et al., 2020). In the Himalayan region, studies on ionic chemical characteristics have focused on the snow cover dynamic (He et al., 2001; May et al., 2018). For example, the concentrations of K^+, Mg^{2+}, and Cl^- in snow of the northern Himalayas were much higher than those in the south (Kang et al., 2004). The concentrations of Cl^- and Na^+ in fresh snow on Xixabangma were lower than those of remote regions, such as Amsterdam Island in the Indian Ocean (Galloway et al., 1982). However, for Northwest China, research has mainly focused on glacial areas where chemical information is well preserved. Furthermore, any analysis of the chemical properties of snowpack in a single area does not represent the entirety of Northwest China. Therefore, we selected the Altay region in northern Xinjiang and the Heihe region in the northern margin of the Tibetan Plateau as study areas, where there are large differences in topography and climate, aiming to reveal the origin and interannual variation of snow chemical composition in typical snow cover areas in Northwest China and determine the impact of the atmospheric circulation system on regional environments.

Northwest China has a large area, and there are great differences in geographical conditions and climatic environment, resulting in regionally different sources and characteristics of the main water-soluble inorganic ions in snow (Church et al., 1982; Keene et al., 1986). In the East Tianshan Mountains, Williams et al. (1992) revealed the reason for the higher pH value of the new snow, and You and Dong (2011) summarized the characteristics of atmospheric dust deposition in snow. So far, the source and post-deposition process of chemical substances in snow have been made clear (Filippa et al., 2010; Li et al., 2015a; Li Q. et al., 2017; Panicker et al., 2019; Thapa et al., 2020; Wei et al., 2020). However, less attention has been paid to the distribution and source of seasonal snow in East Asia, especially in Northwest China. Therefore, due to the short lifetime of most pollutants in the atmosphere and the wide spatial distribution of snowfall in Northwest China, mechanisms and potential sources of air pollutants have not yet been fully understood (Zhang et al., 2013).

In summary, to quantify the main water-soluble inorganic ions in seasonal snow in Northwest China and reveal their natural or anthropogenic sources, this study took Northwest China as the study area and analyzed snow samples collected in the Altay and Heihe regions during two snow seasons from 2018 to 2020. This study further revealed the composition and spatial and temporal distribution characteristics of water-soluble inorganic ions in snow in Northwest China. In addition, the sources and interannual variations of chemical ions in snow cover were discussed to provide basic data for subsequent studies of the stable snow cover area in Northwest China.

2 Materials and methods

2.1 Study area

Northwest China is far inland, surrounded by vast deserts and Gobi sandy beaches. Because of the obstruction of the plateau and mountains to the humid air flow, the climate is characterized as being arid with low precipitation. Snow samples were collected from both northern Xinjiang and the northeastern Tibetan Plateau (Figure 1). The sampling site in northern Xinjiang (89°37′E, 46°57′N, 941 m a.s.l.) was located in the eastern end of the Altay region, near the Altay Mountain Glacial Snow and Environment Observation and Research Station at the southern foot of the Altay Mountains and the northern margin of the Junggar Basin. It has a temperate continental climate characterized by hot and dry summers, snowy and cold winters, and large annual temperature variations. Altay has large elevation differences and is adjacent to Russia, Kazakhstan, and Mongolia. The annual average precipitation in Altay is 150–200 mm, which is mainly concentrated in mountainous areas, accounting for more than 80% of the total annual precipitation (Li et al., 2015b). The average snowfall in winter in Northern Xinjiang is 94.6 mm, and that in the Altay region is more than 200 mm (Yang et al., 2017). The sampling site in the northeastern Tibetan Plateau (100°14′E, 38°0′N, 4,103 m a.s.l.) was located in the middle of the Qilian Mountains and the upper reaches of the Heihe River Basin, near the Heihe Remote Sensing Experimental Research Station. Its average altitude is over 3,000 m, the annual average temperature is about 1°C, and the annual precipitation is about 420 mm, belonging to a typical plateau continental climate. The site has the characteristics of wet in summer, dry and cold in winter and a large annual temperature variation. The unique geographical location, complex topography, and diverse climate types in Northwest China make the study of snow and ice chemistry in this region of more important environmental significance and ecological value.

2.2 Sample collection and analysis

Samples were collected at fixed locations weekly for two snow seasons, from 7 November 2018 to 20 March 2019 and from 9 November 2019 to 29 April 2020. In Heihe and Altay, 53 and 57 surface snow samples and 142 and 186 snow pit samples were collected, respectively (Table 1). The sampling points were selected in an open and flat place far away from cities to avoid human activity (Wang et al., 2015), and the longitude, latitude, and elevation of the sampling points were measured *via* GPS. Masks and PVC gloves were worn throughout the sampling to prevent contamination. The snow samples were stratified, and one sample was collected every 5 cm from bottom to top. The collected snow samples were placed in a Whirl-Pak Ziplock bag, and the air was discharged cleanly. The volume of each sample was about 800 mL. The samples were at −18°C before processing and analysis.

All snow samples were tested at the Shaanxi Key Laboratory of Earth Surface System and Environmental Carrying Capacity. The snow samples were allowed to melt in an ultra-clean laboratory at room temperature before testing. To avoid contamination from the air, the experiment was carried out immediately after melting. The samples were filtered by a Polyether sulfone (PES) filter with a pore size of 0.22 μm. The pH and electrical conductivity (EC) of the samples were determined by a portable pH meter (Five Easy Plus™, Mettler Toledo, Switzerland) and a conductivity meter (Seven2Go™, Mettler Toledo, Switzerland), respectively. The anions and cations were analyzed by an ion

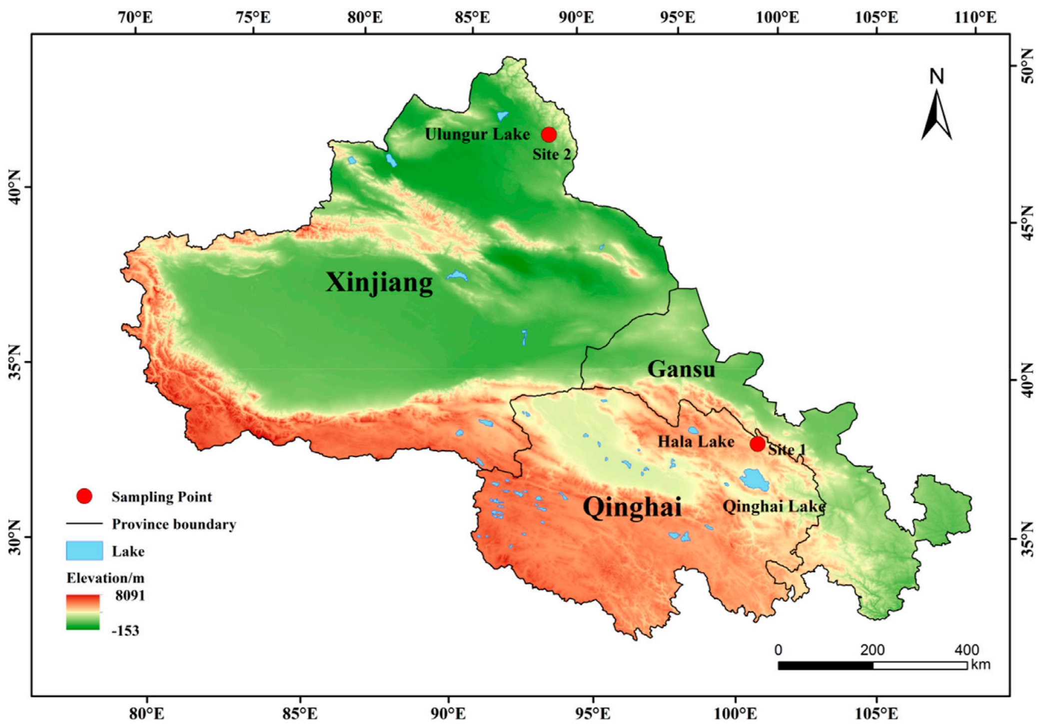

FIGURE 1
The study area and the location of sampling sites. Site 1 and site 2 are the sampling points near Heihe Remote Sensing Experimental Research Station and Altay Mountain Glacial Snow and Environment Observation and Research Station, respectively.

TABLE 1 Sampling information.

Sampling point	Type	Sampling date	Numbers	Longitude and latitude	Elevation (m a.s.l.)
Heihe region	Surface snow	7 November 2018–29 April 2020	53	89°37′ E, 46°57′ N	941
	Snowpit[a]	7 November 2018–29 April 2020	142		
Altay region	Surface snow	23 January 2019–17 March 2020	57	100°14′ E, 38°0′ N	4,103
	Snowpit[a]	23 January 2019–17 March 2020	186		

[a]The depth of the snow pit is about 20–50 cm.

chromatograph (IC, Dionex-AQ, US). The separation of cations and anions was achieved *via* Dionex IonPac CS12A (4 mm × 250 mm) and Dionex IonPac AS11-HC (4 mm × 250 mm) analytical columns, respectively. In addition, Dionex IonPac CG12A (4 mm × 50 mm) and Dionex IonPac AG11-HC (4 mm × 50 mm) columns were used as guard columns for cations and anions, respectively. The chromatography columns were kept at 30°C during measurements. The mobile phases of the cation and anion IC system were 20 mmol/L methane sulfonic acid and 30 mmol/L potassium hydroxide solution, respectively, all under a flow rate of 1 min/s. Standard single-cation (Ca^{2+}, Na^+, K^+, Mg^{2+}, and NH_4^+, 1,000 mg/L) and single-anion (SO_4^{2-}, NO_3^-, and Cl^-, 1,000 mg/L) solutions were obtained from National Non-ferrous Metals and Electronic Materials Analysis and Testing Center, Beijing, China. The analytical standard deviation is less than 5%, and the measurement accuracy is 1 ng/g. All samples were analyzed randomly 2–3 times. The test values for the individual samples were then averaged, yielding an estimated error in ion concentration of ≤10%.

2.3 Research methods

Correlation analysis and enrichment factor were considered to be important methods to determine the source of ions in snow and ice (Haeberli et al., 1988; Sundriyal et al., 2018). In order to more accurately determine the source of the elements to be measured, the enrichment factor (EF) method (Okay et al., 2002; Cao et al., 2009) was adopted. The key of this method was the selection of sea-salt tracer ions (Church et al., 1982; Keene et al., 1986; Zhang et al., 2012) with following rules.

(1) If the equivalent ratios of Cl^-/Na^+ and Mg^{2+}/Na^+ concentrations are greater than those of standard seawater ($Cl^-/Na^+ = 1.17$, $Mg^{2+}/Na^+ = 0.23$), then Na^+ can be used as the sea-salt tracer ion.
(2) If the equivalent ratios of Na^+/Cl^- and Mg^{2+}/Cl^- concentrations are greater than those of standard seawater ($Na^+/Cl^- = 0.86$, $Mg^{2+}/Cl^- = 0.20$), then Cl^- can be used as the sea-salt tracer ion.

TABLE 2 The concentration of main water-soluble inorganic ions in snow from Heihe (HH) and Altay (ALT).

Year		2018/2019				2019/2020			
Element	SP	Max	Min	Ave	STD	Max	Min	Ave	STD
Na^+(mg·L^{-1})	HH	2.30	0.08	0.85	0.50	10.69	0.01	0.92	1.47
	ALT	2.31	0.28	0.88	0.48	3.70	0.02	0.51	0.58
NH_4^+(mg·L^{-1})	HH	0.92	0.31	0.55	0.13	0.59	0.27	0.27	0.11
	ALT	1.61	0.29	0.87	0.31	2.12	0.16	0.72	0.39
K^+(mg·L^{-1})	HH	0.30	0.02	0.09	0.06	3.40	0.04	0.26	0.39
	ALT	1.75	0.07	0.31	0.30	3.00	0.05	0.27	0.39
Mg^{2+}(mg·L^{-1})	HH	0.54	0.03	0.15	0.08	4.25	0.04	0.42	0.56
	ALT	2.15	0.13	0.69	0.51	2.54	0.05	0.45	0.41
Ca^{2+}(mg·L^{-1})	HH	7.25	0.50	3.02	1.53	22.25	0.09	3.34	3.46
	ALT	12.59	1.92	4.65	2.67	12.79	0.26	2.81	2.21
Σ^+	HH	4.66				5.21			
	ALT	7.40				4.76			
Cl^-(mg·L^{-1})	HH	2.49	0.08	0.72	0.44	10.87	0.05	1.16	1.63
	ALT	2.01	0.36	0.84	0.37	2.13	0.02	0.50	0.37
SO_4^{2-}(mg·L^{-1})	HH	5.67	0.16	1.86	1.33	12.31	0.07	0.91	1.54
	ALT	19.91	0.57	4.50	5.11	19.12	0.07	1.46	2.63
NO_3^-(mg·L^{-1})	HH	1.73	0.07	0.71	0.31	3.08	0.03	0.55	0.57
	ALT	8.54	0.31	1.70	1.94	17.91	0.16	2.73	2.44
Σ^-	HH	3.29				2.62			
	ALT	7.04				4.69			
Σ^++Σ^-	HH	7.95				7.83			
	ALT	14.44				9.45			
pH	HH	9.42	6.44	7.45	0.57	9.03	6.06	7.13	0.55
	ALT	7.83	6.40	6.99	0.31	8.82	5.43	6.93	0.42

(3) If the equivalent ratios of Na^+/Mg^{2+} and Cl^-/Mg^{2+} concentrations are greater than those of standard seawater ($Na^+/Mg^{2+} = 4.40$, $Cl^-/Mg^{2+} = 5.13$), then Mg^{2+} can be used as the sea-salt tracer ion.

Finally, Cl^- was selected as the sea-salt tracer ion, and the ratios of different ions in the ocean obtained by Keene et al. (1986) were used to determine. Ca^{2+} was selected as the reference element of crustal source (Taylor, 1964).

To further understand the composition of different sources of various ions, the relative contributions of sea-salt fraction, crustal fraction, and anthropogenic sources fraction were calculated using the following formula:

$$EF_{seawater} = (X/Cl^-)_{sample} \big/ (X/Cl^-)_{seawater} \quad (1)$$

$$EF_{crustal} = (X/Ca^{2+})_{sample} \big/ (X/Ca^{2+})_{crustal} \quad (2)$$

$$SSF(\%) = \frac{(X/Cl^-)_{seawater}}{(X/Cl^-)_{sample}} \times 100\% \quad (3)$$

$$CF(\%) = \frac{(X/Ca^{2+})_{seawater}}{(X/Ca^{2+})_{sample}} \times 100\% \quad (4)$$

$$AF(\%) = 1 - SSF(\%) - CF(\%) \quad (5)$$

Where X is the ion concentration to be measured. In general, elements with EF significantly higher than 1.00 are considered to be enriched relative to the reference source, otherwise are diluted. SSF, CF and ASF refer to Sea-salt Fraction, Crustal Fraction and Anthropogenic Fraction, respectively.

To further trace the potential source areas and transport paths of chemical ions and dust particles in the snow in the study area, the HYSPLIT (Hybrid Single Practical Lagrangian Integrated Trajectory) model developed by NOAA Air Resources Laboratory (http://www.noaa.gov) was also used in this study. The initial height of the trajectory was chosen to be 500 m above the sampling point, and the backward air mass trajectory was pushed back for 3 days. The meteorological data needed for the model calculation came from the National Center for

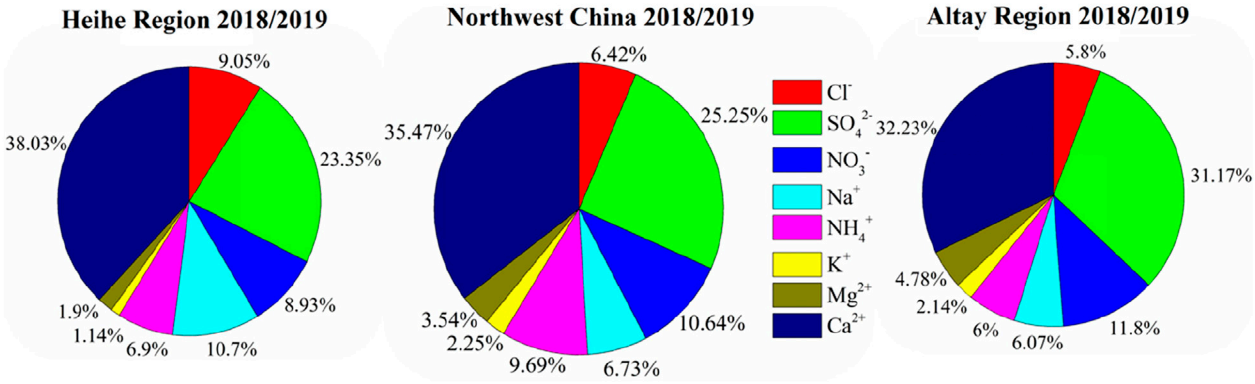

FIGURE 2
The proportion of ion concentration in Heihe region, Altay region and Northwest China region in 2018/2019.

Environmental Prediction (NCEP) and the National Center for Atmospheric Research (NCAR), and the spatial resolution of the data was 1° × 1°.

3 Results and discussion

3.1 Chemical characteristics of ions in snow

To some extent, the chemical information recorded in snow can reflect the level of air pollution and climate conditions (Wang P. et al., 2008). Table 2 shows the concentration of water-soluble inorganic ions, pH, and EC values of snow during two snow seasons in Northwest China. It was found that the pH values of snow in Heihe and Altay in 2018/2019 were 6.44–9.42 and 6.40–7.83, with averages of 7.45 and 6.99, respectively. The pH values of snow in Heihe and Altay in 2019/2020 were 6.06–9.03 and 5.43–8.82, with averages of 7.13 and 6.93, respectively. The pH was higher than previous reported values from different locations, such as 6.74 in Tianjin (Wu et al., 2016), China, 5.50 in the Tianshan Mountains (Li et al., 2010), and 5.90 in snow from Himalayan glaciers (Panicker et al., 2019). Previous studies have shown that Ca^{2+} is a key ion affecting the pH of snow (Li et al., 2007; Rao et al., 2019). Acidic ions in snow are neutralized by alkaline ions such as Ca^{2+} and NH_4^+ (Rao et al., 2019; Liu et al., 2020). It is highly possible that the high pH value of snow in this study was related to the vast saline-alkali soil in Northwest China and frequent high-flux dust weather.

Due to the influence of topography and atmospheric circulation, the concentration of water-soluble inorganic ions in snow varies greatly in different regions. In this study, the concentration sum of cations (Σ^+) was higher than that of anions (Σ^-). Spatially, the total ion concentration of snow in Altay was higher than that in Heihe. The lower the elevation of the sampling site, the more strongly it can be affected by dust from nearby sources; and the closer it is to the dust source, the more strongly it can be affected by westerly winds. Temporally, the total ion concentration of snow in 2018/2019 was higher than in 2019/2020. The imbalance between the concentrations of anions and cations indicated that in addition to the inorganic anions analyzed in this study, other anions (e.g., CO_3^{2-} and HCO_3^-) also contributed significantly (Kim and Cho, 2003). Previous studies have shown that concentration differences between anions and cations in snow can reflect the concentration values of CO_3^{2-} and HCO_3^-, where excess cations may come from the surrounding soil dust (Wake et al., 1993; Li et al., 2019).

The sequencing results (Figures 2, 3) showed that Ca^{2+} was the dominant cation, which may be related to the arid and semi-arid dust area in Northwest China close to central Asia; the order of cation concentrations was $Ca^{2+} > Na^+ > Mg^{2+} > K^+$, which was basically consistent with the order of crustal elements ($Ca^{2+} > Na^+ > K^+ > Mg^{2+}$), indicating mainly terrestrial sources. In 2018/2019, SO_4^{2-} was the dominant anion in snow in both areas, accounting for 25.25% of the total ion concentration. In 2019/2020, Cl^- and NO_3^- were the main anions in the snow in the Heihe and Altay regions, accounting for 14.7% and 29.02% of the total ion concentration, respectively, and NH_4^+ and NO_3^- concentrations increased significantly compared with those in 2018/2019. The major ions in snow around the world are different. For example, the main cation and anion in snow from Northwest China (Li et al., 2010; Wang et al., 2016), central Japan (Dong et al., 2011; Kawamura et al., 2012), and the Satopunath Glacier of the Himalayas (Panicker et al., 2019) were Ca^{2+} and SO_4^{2-}, respectively. Na^+ and Cl^- were the major cations and anions in snow from Wasatch Mountain in Utah, western United States, respectively (Hall et al., 2014).

Upon comparing the ion concentration of the two areas, the concentrations of SO_4^{2-} and NO_3^- in the Altay region were much higher than that in the Heihe region, whereas the concentrations of Cl^- and Na^+ showed the opposite trend. This is because the Altay region is a relatively well-developed region in Xinjiang and even in Northwest China; bordering Russia and other countries, is the main route for the circulation of goods. Compared with the Heihe region, the population density of Altay is higher, and industry is more developed. Coal, coke oven gas, and traffic fuel are important pollution sources in Xinjiang, China (Turap et al., 2019; Yu et al., 2019). When the westerly circulation passes through many petroleum industrial areas and urban agglomeration in Xinjiang, SO_4^{2-} and NO_3^- become enriched in the snow. In contrast, the Heihe region is located in the northeastern Tibetan Plateau, close to the Qaidam Basin and surrounded by many large and small salt lakes such as Qinghai Lake and Hala Lake. The content of Cl^- and Na^+ was high due to the input of salt mineral dust and salt lake materials (Li et al., 2015c; He et al., 2019).

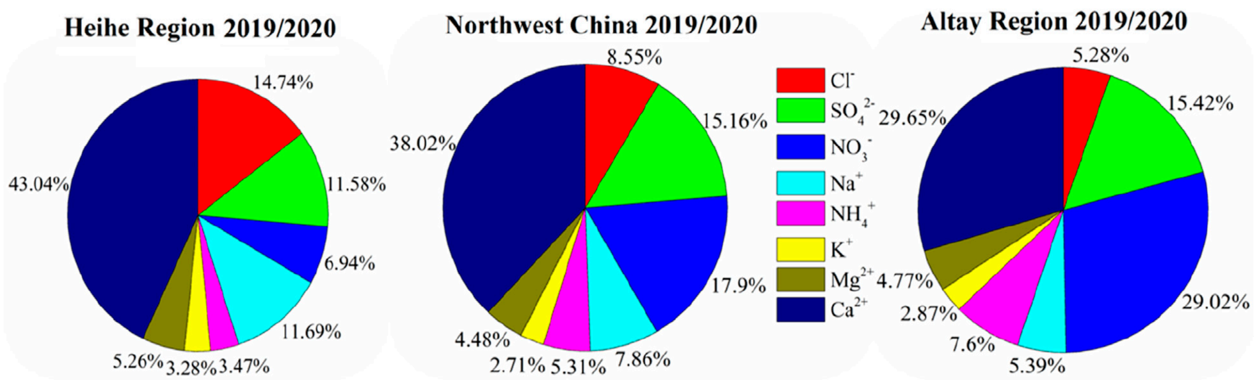

FIGURE 3
The proportion of ion concentration in Heihe region, Altay region and Northwest China region in 2019/2020.

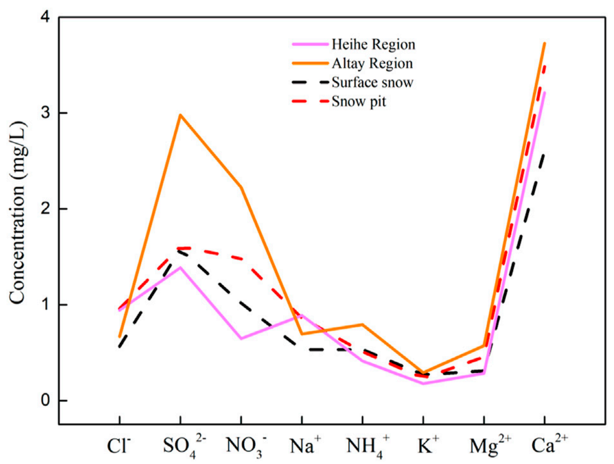

FIGURE 4
Comparison of mean values of ion concentrations in snow from different regions and types of samples. The black and red dotted lines are the average values of ion concentrations in surface snow samples and snow pits, respectively. The pink and orange solid lines are the average values of ion concentrations in snow in Heihe and Altay, respectively.

The average NH_4^+ concentration in the Altay region was higher than that in the Heihe region during the two consecutive snow accumulation periods (0.85 mg L^{-1} > 0.55 mg L^{-1}; 0.72 mg L^{-1} > 0.27 mg L^{-1}). Research has shown that NH_4^+ is not only derived from agricultural activities but also from vehicle exhaust emissions (Bo et al., 2019). This is because automobile exhaust catalytic converters produce NH_3 when converting CO and NO_x, and NH_3 is mainly generated in the process of vehicle acceleration (Gandhi et al., 1991; Huai et al., 2003; Burgard et al., 2006). The Altay region is more prosperous than the Heihe region in terms of tourism, industry, and urbanization, so the chemicals in the snow are a direct result of human activities.

In addition to the atmospheric circulation pathway, other factors such as the different sources of water vapor and the post-deposition process of snowpack can also affect the ion concentration in snow pits and surface snow. In this work, the average value of each ion concentration in surface snow was generally lower than that in snow pit (Figure 4). The vertical distribution of ion concentration may be due to the fact that surface snow represents recent precipitation events, whereas snow in snow pits represents precipitation over a longer period of time after atmospheric chemical deposition (Liu et al., 2020).

3.2 Spatial and temporal distribution characteristics of ion concentration

3.2.1 Temporal distribution characteristics of ion concentration

The ions in snow and ice are not only determined by geographical environment; atmospheric circulation is also crucial. Figure 5 shows the change of ion concentration in snow in the Altay and Heihe regions during two snow seasons from 2018 to 2020. Compared with 2018/2019, the ion concentration decreased slightly in 2019/2020, and the depletion of ion concentration in the Altay region was larger. Ca^{2+}, SO_4^{2-}, Cl^-, and Na^+ decreased in the Altay region compared with the previous year, whereas K^+ increased. However, SO_4^{2-} and NH_4^+ in the Heihe area decreased significantly compared with the previous year; and Ca^{2+}, Cl^-, Na^+, K^+, and Mg^{2+} increased slightly. It is generally believed that Ca^{2+} comes from insoluble $CaCO_3$ in dust in arid and semi-arid areas (Wake et al., 1993; Li et al., 2005; Sun et al., 2010), which is related to the amount of terrestrial material input. However, Northwest China is close to the dust source area of Central Asia, so the proportion of Ca^{2+} is the largest.

Previous research has shown that temperature, precipitation, wind speed, and other factors affect the concentration of ions in snow (Li et al., 2010). The concentration of SO_2 and NO_2 in the atmosphere can reflect the concentration of SO_4^{2-} and NO_3^- in snow. Observations of SO_2 and NO_2 in the atmosphere of the Altay region (Figure 6A) during the sampling period indicated that the concentration of SO_2 in 2018/2019 was higher than that in 2019/2020, whereas NO_2 showed the opposite trend. This result is consistent with the conclusion of SO_4^{2-} and NO_3^- shown in Figure 5. Combined with the precipitation data of Qilian Station and Altay Station, as well as China's national meteorological ground observation stations near the study area (Figure 6B), the results showed that the average monthly precipitation in the Heihe region during the two consecutive winter sampling periods was small, as was its difference between periods. In

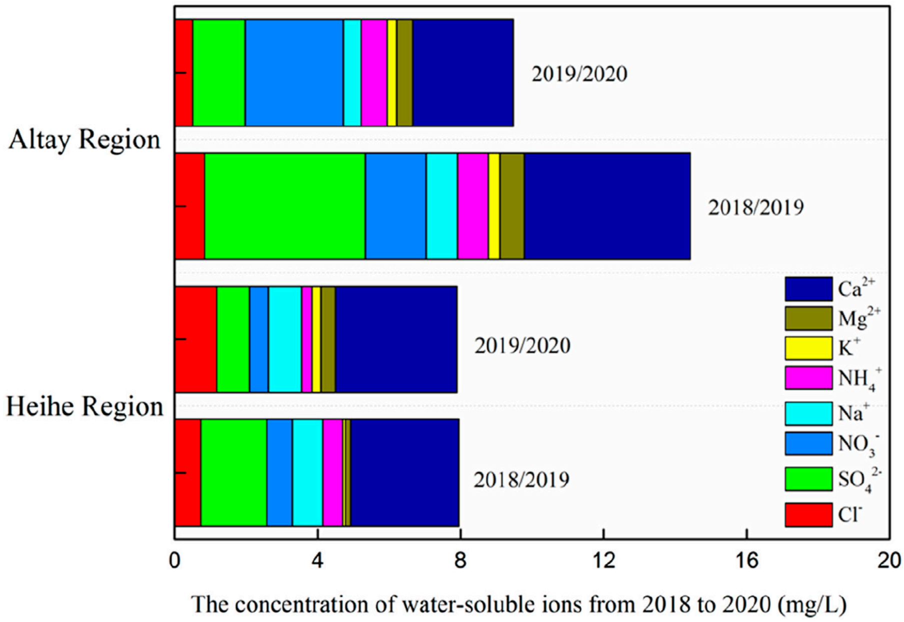

FIGURE 5
Interannual variations of several major inorganic ions in snowpack in Heihe and Altay regions during 2018–2020.

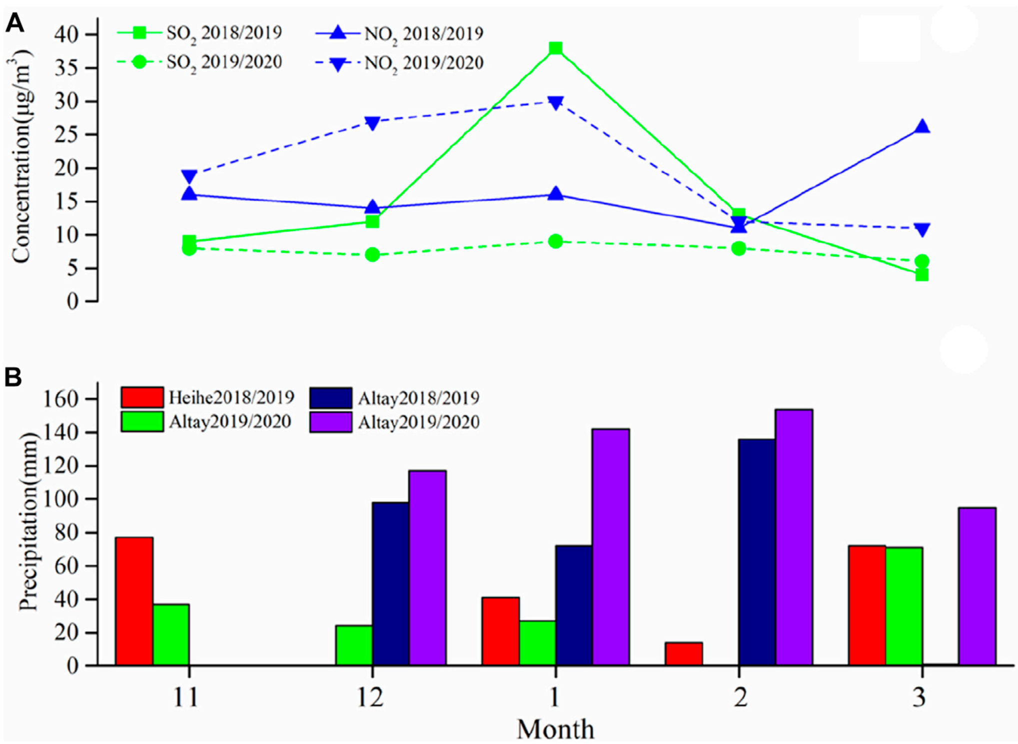

FIGURE 6
(A) is the change in concentration of SO_2 and NO_2 in the air during the sampling period in Altay region. The solid line is 2018/2019 and the dotted line is 2019/2020. **(B)** is the average value of monthly precipitation in the study area during the sampling period. The average value of monthly precipitation in December 2018 and February 2020 is 0 in Heihe area. The datas comes from the China Meteorological Administration (http://data.cma.cn/).

contrast, the average monthly precipitation in the Altay region in winter 2019/2020 was greater than that in winter 2018/2019. In dry and cold environments, the air mass passes through dust sources and carries the sand and dust to the downwind areas, leading to frequent sandstorms. In contrast, in warm and humid environments, precipitation removes dust particles from the air and reduces

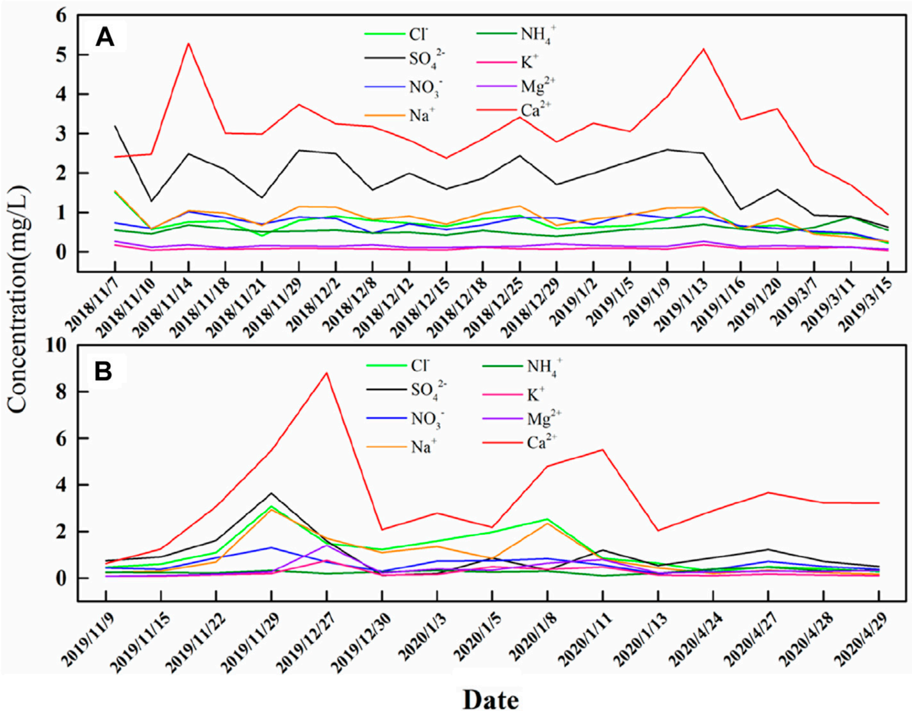

FIGURE 7
Temporal variation of several major inorganic ions in Heihe region, where **(A)** is in 2018/2019, and **(B)** is in 2019/2020.

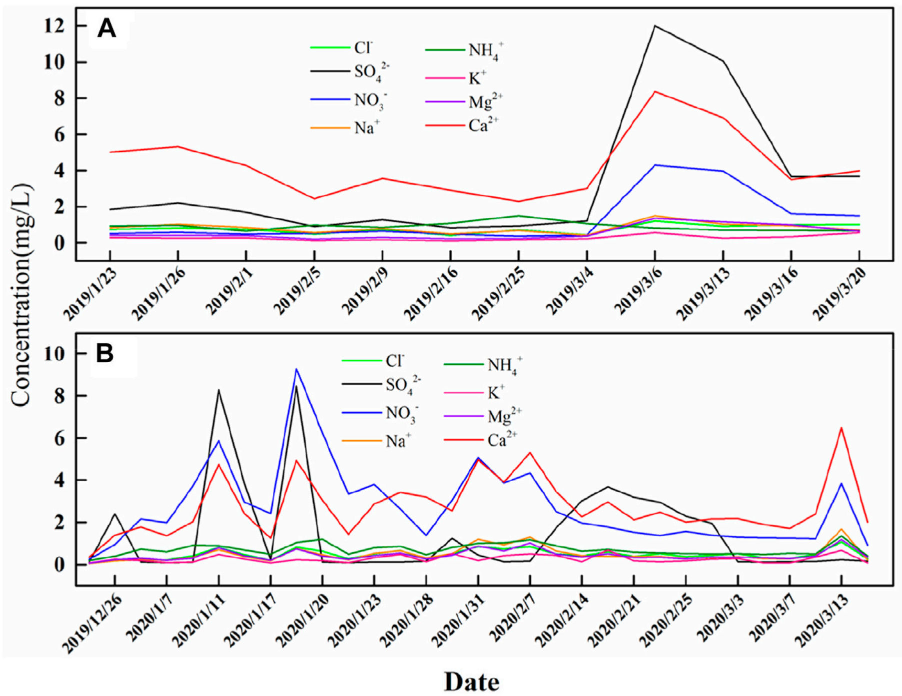

FIGURE 8
Temporal variation of several major inorganic ions in Altay region, where **(A)** is in 2018/2019, and **(B)** is in 2019/2020.

atmospheric aerosol concentrations (Wang Y. et al., 2008; Kang et al., 2022). Therefore, the concentration of ions in the winter of 2018/2019 in the Altay region snow was higher than that in the winter of 2019/2020, and precipitation was one of the important factors. In addition, the COVID-19 outbreak in the winter of 2019/2020, which led to the closure of factories and enterprises across China's Xinjiang

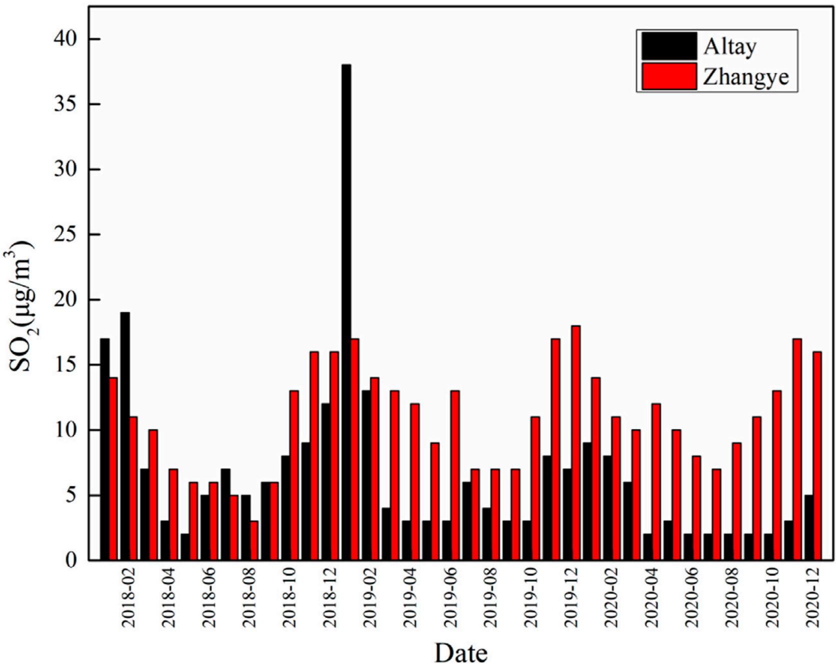

FIGURE 9
Monthly average value of SO_2 concentration in the atmosphere of Altay and Zhangye regions from 2018 to 2020. Among them, Zhangye is selected as the meteorological station near the Heihe sampling point. The data come from the China Meteorological Administration (http://data.cma.cn/).

region, may also have contributed to the decrease in atmospheric aerosol content.

Both the atmospheric scavenging effect of snowfall and the input of dust particles from the ground increase the concentration of ions in snow, resulting in a strong correlation with dust activity. To understand their temporal variation characteristics, the ion concentrations of snow samples in the two areas were arranged in chronological order (Figures 7, 8). The concentrations of Ca^{2+}, SO_4^{2-}, Cl^-, and Na^+ during the two snow seasons in the Heihe region showed a consistent trend, whereas the changes of the concentrations of other ions were relatively small, indicating that the source and migration of ions in the dry season had a strong consistency. In the beginning of November, the ion concentration increased significantly, which may be due to the fact that there were many deserts (e.g., the Taklimakan Desert and the Gurbantunggut Desert) and Gobi areas distributed near the two places, where the strong wind blew terrestrial materials and deposited them in the snow. Another reason may be that pollutants in the air were removed by snowfall. In addition, due to the influence of the underlying surface, the bottom air cooled rapidly in winter, and the inversion layer readily appeared at low altitude. The pollutants in the air were confined in the shallow atmosphere and gradually accumulated (Xu et al., 2008; Zhao et al., 2008).

Aerosols from coal and biomass combustion are important sources of air pollution. However, due to the low utilization rate of solid fuels for civil use, they are usually not fully burned, which seriously pollutes the atmosphere (Li et al., 2008). The amount of particulate matter emitted by civil coal combustion is about 100 times higher than that emitted by industrial boilers (Zhang et al., 2017). Moreover, Northwest China still uses coal for heating in winter. In addition to elemental sulfur, sulfur in coal is mainly composed of organic sulfur and inorganic sulfur. During the combustion of coal, all the combustible sulfur is heated and released. In an oxidizing environment, combustible sulfur is oxidized to form SO_2. As shown in Figure 9, we determined the monthly average of SO_2 in the air of the study areas for 2 consecutive years. It was found that the concentration of SO_2 in the air was higher in winter than in other seasons, which may be related to industrial and residential coal-burning in winter. It was observed that the impact of coal combustion on air aerosol in winter was also significant. Similarly, the variation trend of ion concentration in snow in the Altay region

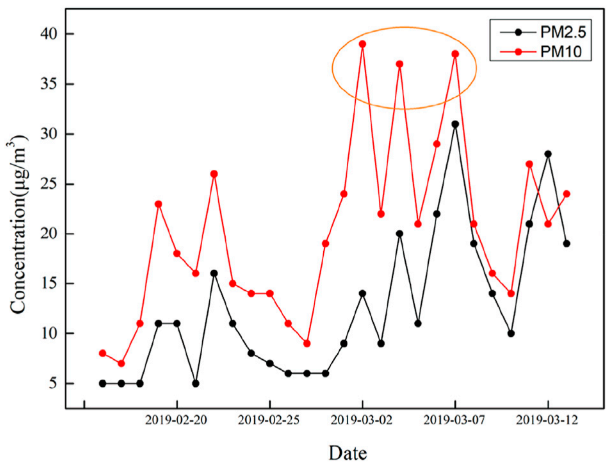

FIGURE 10
The daily average values of PM2.5 and PM10 in Altay region from the end of February to the beginning of March 2019. The data come from the China Meteorological Administration (http://data.cma.cn/).

TABLE 3 Comparison of ion concentration between the study area and other typical snow cover areas.

Study areas	Period of study	Type	Ion concentration (mg·L^{-1})								References
			Na^+	NH_4^+	K^+	Mg^{2+}	Ca^{2+}	Cl^-	SO_4^{2-}	NO_3^-	
Heihe region	2018–2020	Snow pit	0.89	0.41	0.18	0.29	3.18	0.94	1.39	0.63	In this study
Altay region	2018–2020	Snow pit	0.70	0.80	0.29	0.57	3.73	0.67	2.98	2.22	In this study
Northeast China	2017–2018	Fresh snow	2.25	2.63	1.06	1.05	10.39	2.99	6.97	3.34	Xue et al. (2020)
Primorsky Krai, Russia	2012–2013	Snowpack	2.7	-	0.8	0.4	2.5	5.2	4.9	3.4	Kondrat'ev et al. (2017)
The Alps	2017	Snow pit	0.017	0.026	-	-	0.071	0.034	0.057	0.25	Avak et al. (2019)
The Satopnath Glacier, Himalayas	2016	Fresh and old snow	0.12	0.018	0.12	0.16	0.48	0.17	0.18	0.05	Panicker et al. (2019)
Tianshan No.1 Glacier	2004–2005	Snowpack	0.074	0.17	0.042	0.13	1.49	0.26	0.55	0.36	Li et al. (2010)
Lao Hugou No.12 Glacier	2006	Snow pit	0.87	0.36	0.087	0.17	2.88	1.29	1.50	0.55	Cui et al. (2011)
Baishui No.1 Glacier	2006	Fresh snow	0.18	-	0.19	0.23	1.83	0.19	0.55	0.15	Zhang et al. (2010)
Alert, Arctic	2014–2015	Fresh snow	0.11	0.012	0.014	0.043	0.19	0.24	0.31	0.14	Macdonald et al. (2017)

was consistent, but that in winter 2019/2020 was relatively large, which may be related to frequent local dust activities.

An ion concentration maximum occurred in early March 2019, which may be related to the arrival of spring dust season (Osada et al., 2004). Compared with the beginning of the snow season, the concentration of ions increased at first, with the concentration of ions peaking in the middle or later part of the snow season. This phenomenon can be explained by the fact that the accumulated air pollutants were scavenged and deposited into snow (Xue et al., 2020). It is generally believed that the concentration of PM2.5 and PM10 can reflect the concentration of floating dust in the air. We collected the concentration data of PM2.5 and PM10 in the Altay region from the end of February 2019 to the beginning of March 2019 (Figure 10), which showed that PM2.5 and PM10 concentrations in the air reached a high value on March 6. This result agreed well with the peak value of ion concentration in Altay in March 2019. In addition, the rising temperature in spring increased the evaporation of the land surface and aggravated the drought in the study area (Miao et al., 2016).

3.2.2 Spatial distribution characteristics of ion concentration

The difference of geographical environment is often the primary reason for the difference of ion concentration in snow (Church et al., 1982). Moreover, snow and ice chemistry are reliable indicators for monitoring the impact of human activities on the atmospheric environment and can accurately reflect local air pollution (Kuoppamaki et al., 2014; Niu et al., 2020). To further understand the spatial characteristics of ions, ion data of typical snow cover areas in different regions of the world were collected in this paper (Table 3). The ion concentrations in the Altay and Heihe regions were lower than that in other more densely populated and industrially developed areas (e.g., Northeast China and Russia). However, they were basically 1–2 orders of magnitude higher than some high-altitude or high-latitude areas (e.g., the Alps, Satopnath glacier, Tianshan No.1 Glacier, and Alert) and marine glaciers (e.g., Baishui Glacier No.1). NH_4^+ and NO_3^- concentrations usually reflect anthropogenic influences (Kulshrestha et al., 2005; Wang et al., 2005; Xu et al., 2008; Kumar et al., 2016). Among them, the study area, Russia, and Northeast China were more obvious, which may be related to local biomass combustion, fossil fuel combustion, and industrial and vehicle-exhaust emissions. In general, the spatial difference of soluble inorganic ion concentration in snow indicated inorganic ions in snow in the dust source area of Central Asia was higher than that of marine glaciers and remote areas at high altitude or high latitude.

The concentration ratio of anions and cations between the study area and other typical snow cover areas (Figure 11) showed that the cation composition ratio of the study area was close to that of Northeast China, Laohugou No. 12 Glacier, and Baishui No. 1 Glacier, with a large proportion of Ca^{2+}, followed by Mg^{2+}. It is generally believed that Ca^{2+} and Mg^{2+} come from arid areas such as deserts and loess regions in Eurasia (Okada and Kai, 2004). In Primorsky Krai, Russia, the difference in the composition of cations was the largest—probably because the sampling point was close to the ocean, which made the concentrations of Na^+ and K^+ relatively high. The high concentrations of Cl^- and Na^+ brought by marine air masses made this area obviously affected by sea-salt aerosol. However, the composition of anions in different regions was obviously different, with the highest proportion being SO_4^{2-} across all regions. There was a significant difference between the Heihe and Altay regions, where the concentration of Cl^- in snow in the Heihe region was relatively high, and the difference was more obvious in the Alps, which had a high NO_3^- ratio. This result reflects the regional differences of snow and ice chemistry in different environments.

3.3 Correlation analysis and source

Determining the sources of ions in Northwest China is complicated due to the obvious differences in topography and population density. In this study, the sources of ions were analyzed by the enrichment factor method. Enrichment Factor (EF) values are given in Table 4, which lists the contributions of sea-salt, crustal, and

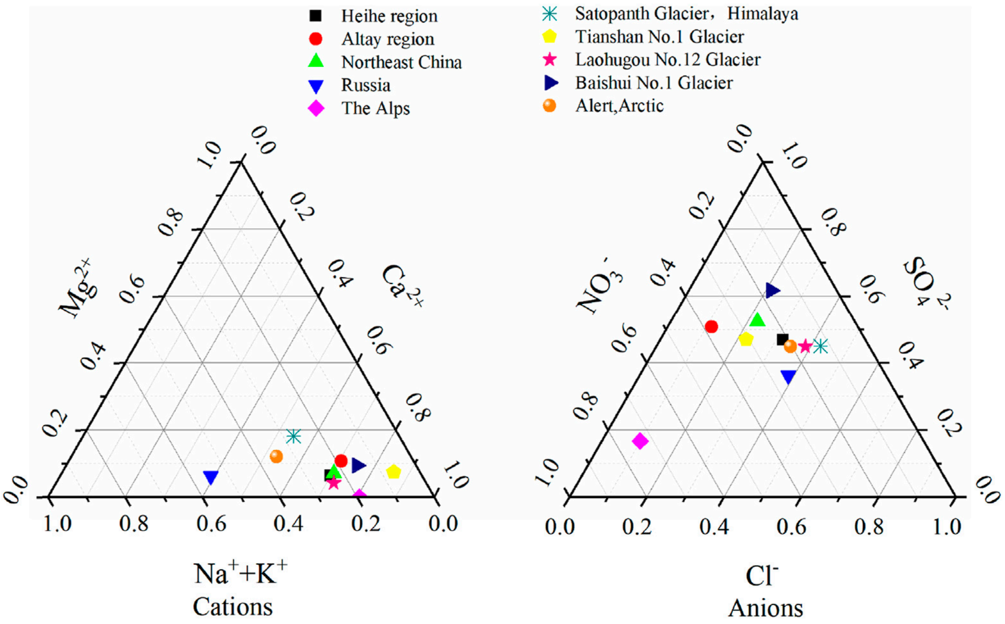

FIGURE 11
Relative proportions of anions and cations between the study area and other typical snow cover areas. $Na^+ + K^+$, Ca^{2+}, and Mg^{2+} are selected as cations. NO_3^-, Cl^-, and SO_4^{2-} are selected as anions.

TABLE 4 Main inorganic ion EF values and the contribution of ion sources in the study area.

Study areas	Elements	Major water-soluble inorganic ions						
		Na^+	K^+	Mg^{2+}	Ca^{2+}	Cl^-	SO_4^{2-}	NO_3^-
Hehei region	$EF_{(seawater)}$	1.70	9.30	4.76	160.53	—	8.97	71.78
	$EF_{(crustal)}$	0.28	0.03	0.96	—	7.67	5.62	22.82
	SSF(%)	58.82	10.75	21.01	0.62	86.96	11.15	1.39
	CF(%)	41.18	89.25	78.99	99.38	13.04	17.79	4.38
	AF (%)	—	—	0.00	—	0.00	71.06	94.23
Altay region	$EF_{(seawater)}$	1.88	21.08	13.11	264.26	—	26.97	354.71
	$EF_{(crustal)}$	0.19	0.04	1.60	—	4.66	10.27	68.58
	SSF(%)	53.19	4.74	7.63	0.38	78.54	3.71	0.28
	CF(%)	46.81	95.26	62.50	99.62	21.46	9.74	1.46
	AF (%)	—	—	29.87	—	0.00	86.55	98.26

anthropogenic fractions to each ion. The $EF_{(seawater)}$ values of all ions were greater than 1, especially Ca^{2+}, indicating that ions were enriched relative to seawater and mainly came from soil. The $EF_{(seawater)}$ and $EF_{(crustal)}$ values of SO_4^{2-} and NO_3^- were both greater than 1, indicating that they were relatively enriched compared to soil and seawater, and NO_3^- was enriched to a higher degree. The $EF_{(crustal)}$ values of K^+ were all much less than 1, indicating that it was mainly from terrestrial sources, with a small proportion of marine sources. Previous studies have shown that K^+ is mainly derived from crustal sources in addition to biomass combustion (Jain et al., 2000; Zhang et al., 2007). Upon further calculating the contribution proportion of ion sources (Table 4), the results showed that Cl^- and Na^+ in snow in the study area were mainly imported from sea sources, but also from land sources, which may be related to the abundant salt dust in the surrounding area (Zheng et al., 2008). However, the AF of Mg^{2+} in snow in the Altay region was 29.87%, which may be related to the burning of coal by residents in winter given the high magnesium content in coal (Zhang et al., 2018).

To further understand the source and transformation of water-soluble inorganic ions in snow, a Pearson correlation analysis was conducted for the main inorganic ions in this study (Figure 12). In general, the correlation coefficients of ions in the Heihe and Altay

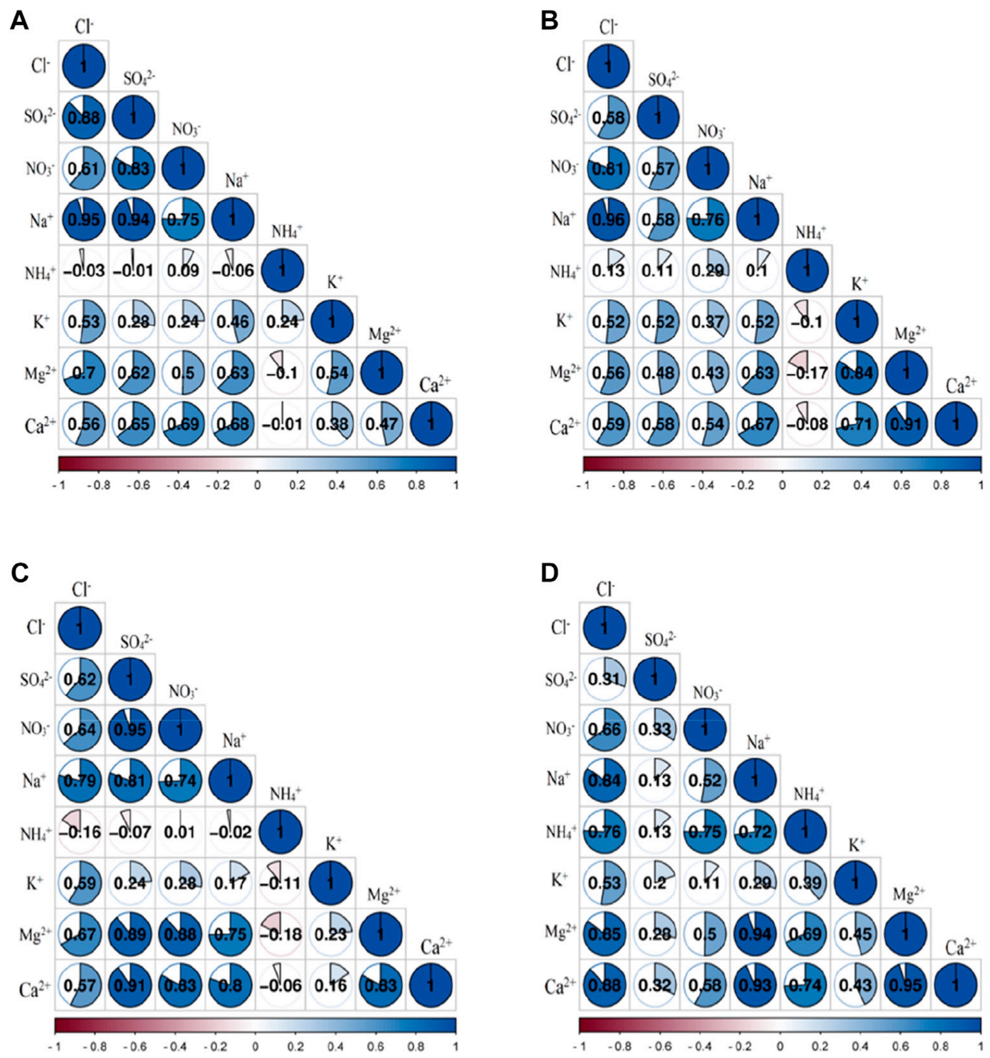

FIGURE 12
Correlation analysis of main inorganic ions in snowpack in the study area, where **(A,B)** are the correlation analysis of ions in 2018/2019 and 2019/2020 in Heihe region, and **(C,D)** are the correlation analysis of ions in 2018/2019 and 2019/2020 in Altay region, respectively.

regions were significantly different during the two snow seasons, indicating different sources. Figures 12A, C show the correlation between ions in snowpack in the Heihe and Altay regions in 2018/2019, respectively. The results of the EF method show that SO_4^{2-} and NO_3^- were driven by anthropogenic sources, and considerable portions of Na^+ and Cl^- were from marine sources. The significant correlation among Cl^-, Na^+, SO_4^{2-}, and NO_3^- indicated that they also had other sources besides anthropogenic and marine ones. Previous studies have shown that an important source of SO_4^{2-} in snow is soil dust, followed by human pollution (Kulshrestha et al., 2003; Kumar et al., 2016). NO_3^- can also be combined with dust to form nitrate substances such as $Ca(NO_3)_2$ and $Mg(NO_3)_2$ (Dentener et al., 1996), and Mg^{2+} is also closely related to dust (Kang et al., 2004). Therefore, the input of mineral dust from numerous salt lakes (e.g., Ulungur Lake, Qinghai Lake, and Hala Lake) and saline-alkali land around Heihe and Altay had certain contributions to Na^+, Mg^{2+}, Cl^-, SO_4^{2-}, and NO_3^-. However, SO_4^{2-} and NO_3^- showed a more significant correlation than other ions, and their AF values were relatively high. SO_4^{2-} may be derived from the combustion of fossil fuels and biomass (Kulshrestha et al., 2005; Kumar et al., 2016), and NO_3^- may come from the photochemical reaction of NO_x emitted from automobile exhaust (Singh et al., 2014).

Figures 12B, D show the correlation between ions in snow cover in the Heihe and Altay regions in 2019/2020, respectively. As mentioned above, Na^+, NO_3^-, Cl^-, Ca^{2+}, Mg^{2+}, and K^+ may come from dust input. Compared with other ions, a weak correlation was seen for NH_4^+. Previous studies have shown that NH_4^+ is mainly derived from terrestrial biological processes and alkaline soil release (e.g., agricultural cultivation and animal feces) (Xu et al., 2008). According to the *Statistical Bulletin of National Economic and Social Development of Altay Region in 2019*, the total sown area of crops in the Altay Region in 2019 was 262,406 ha. Therefore, the significant correlation between NH_4^+ and NO_3^- in this study indicated that NH_4^+ may be related to agricultural sources, existing in the form of NH_4NO_3 aerosol in snow (Kulshrestha et al., 2005). The weak correlation between SO_4^{2-} and other ions in snow in Altay indicated that their sources were different. Given the developed industries in Altay, SO_4^{2-} may be related to acidic gas input generated by factory emissions (Kulshrestha et al., 2003).

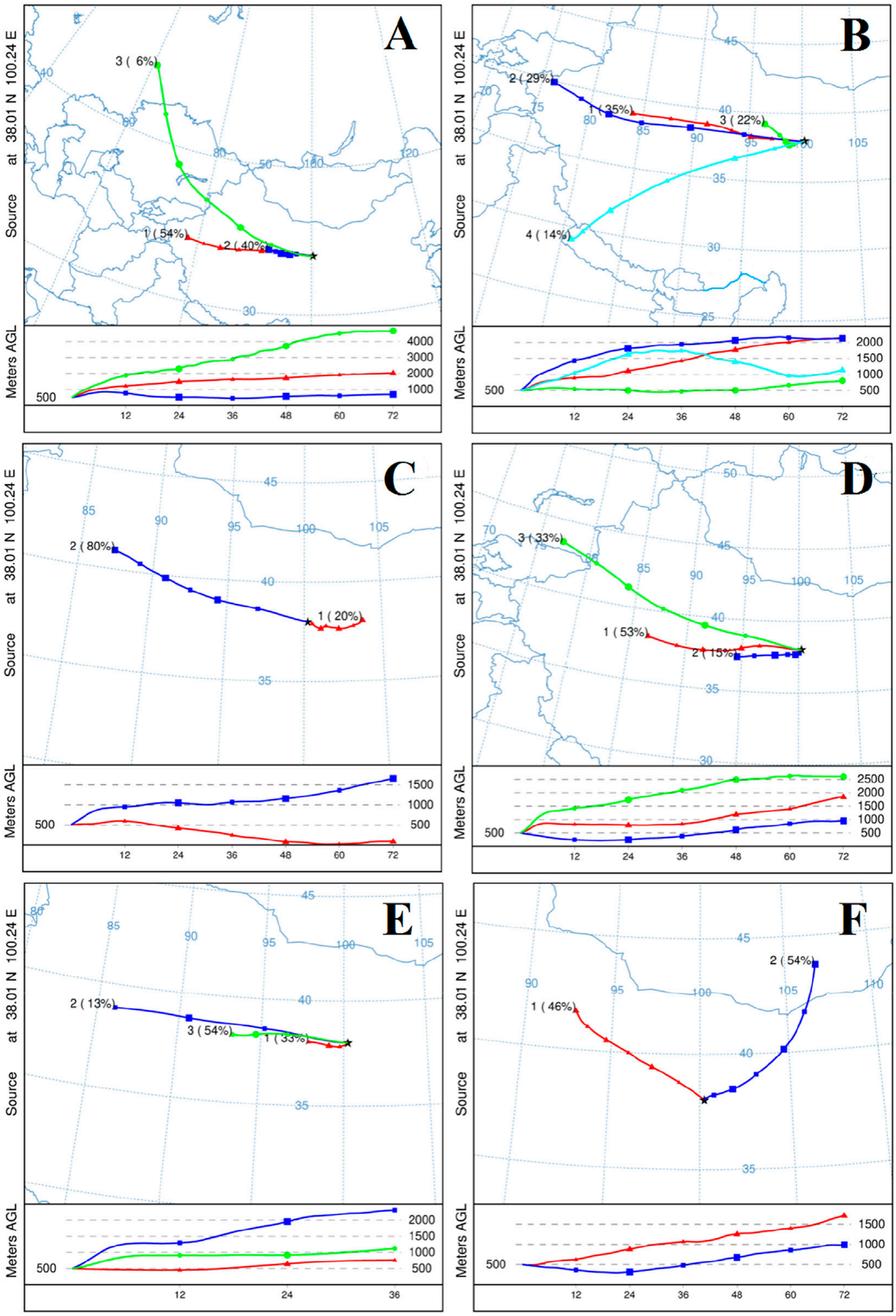

FIGURE 13
Clustering analysis of 72 h backward trajectory of Heihe sampling site, where **(A)** is from November to December 2018; **(B–D)** are January-February, March and November-December 2019, respectively; **(E) (F)** are January-February and April 2020, respectively.

To understand the potential source of water-soluble inorganic ions in snow, the HYSPLIT model was used to simulate the backward trajectory of the air mass 500 m above the sampling point, and the simulation time was divided into three stages according to the time variation characteristics of ion concentration, namely November to December; January to February; March and April (Figures 13, 14). The

10.3389/feart.2023.1099178

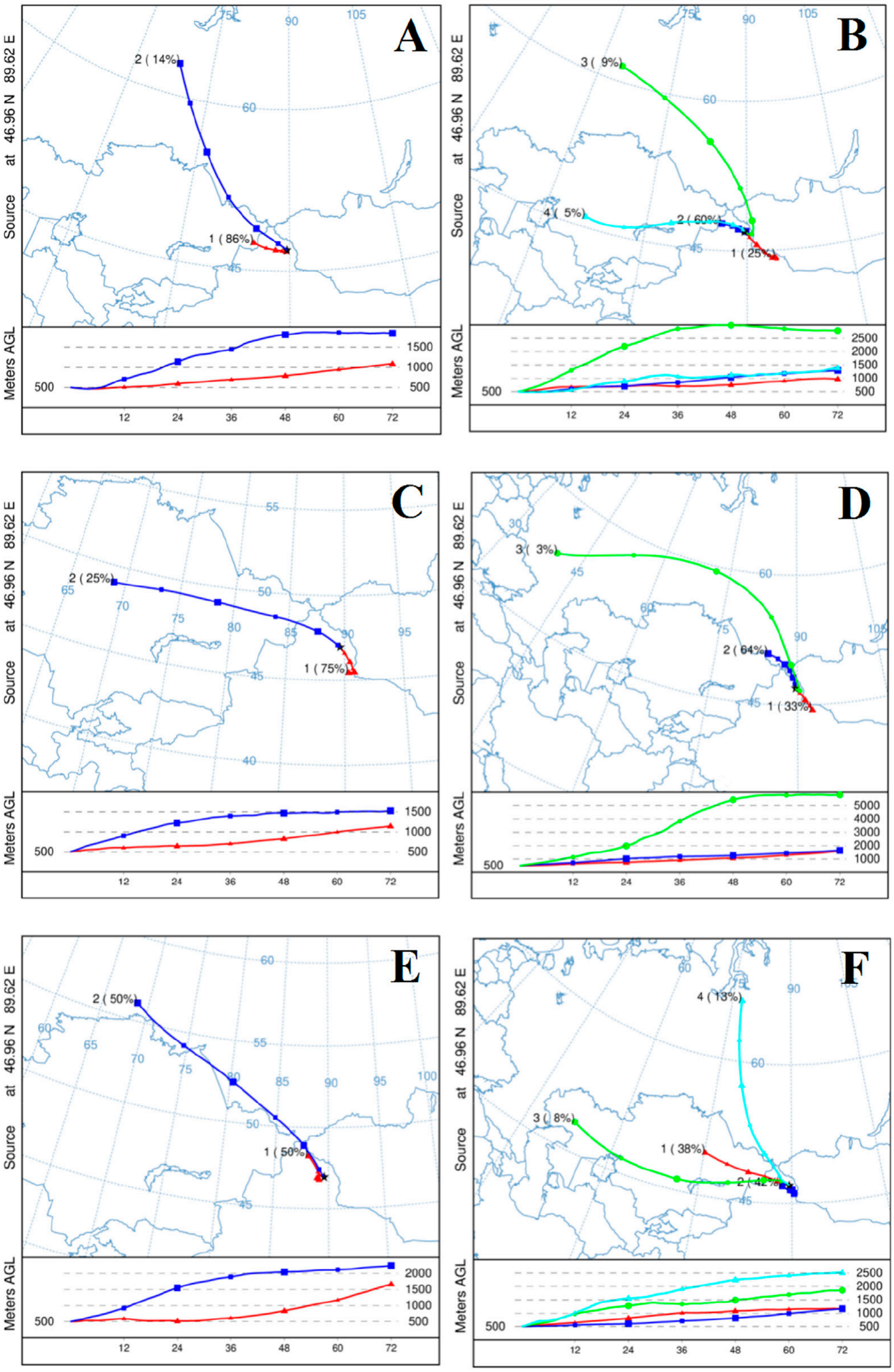

FIGURE 14
Clustering analysis of 72 h backward trajectory of Altay sampling site, where **(A)** is from November to December 2018; **(B–D)** are January-February, March and November-December 2019, respectively; **(E) (F)** are January-February and April 2020, respectively.

results showed that the air mass mainly came from the direction of west to north. In the vertical direction, the air mass mainly showed a gradual sinking movement and was obviously affected by local air mass.

The Heihe region was mainly influenced by air masses from the Taklimakan Desert and the Qaidam Basin in the west. Part of the air mass in the northwest originated from the southern foot of the Ural Mountains. The air mass passed through Kazakhstan and other places, crossed the Tianshan Mountains, and reached the Heihe region. The northeast direction was influenced by the detour flow from the Mongolian Plateau, and the southwest direction was also influenced by the air mass originating from Nepal over the Himalayas. The Altay region was mainly affected by nearby air masses, which was more significant in 2018/2019 compared to 2019/2020. This explained the higher ion concentrations in snow in 2018/2019 than that in 2019/2020. The long-range air masses in the west and northwest originated mainly from central and eastern Kazakhstan and the Russian border, and partly from the southern West Siberian Plain of Russia. In general, air masses passed through arid and semi-arid areas such as deserts and Gobi, carrying large amounts of sand and dust as well as Ca^{2+}, Na^{+}, Cl^{-}, SO_4^{2-}, and other chemicals. In addition, the wind speed was faster in winter and spring, leading to an increase of dust and ions in the snow. Westerly winds may also carry water vapor from Central Asian salt lakes and deserts, increasing the concentration of salts and alkaline metal ions in the snow. The industries in the densely populated areas of Kazakhstan and southern West Siberia are dominated by coal and oil. When the westerly circulation passed through these places, NO_3^{-} and SO_4^{2-} continued to be input along the way and were finally stored in the snow.

4 Conclusion

In this study, water-soluble inorganic ions, pH, and other chemical indexes were measured for snow samples collected from Heihe and Altay, Northwest China during two snow seasons from 2018 to 2020. Here, we focused on the characterization of spatial and temporal variation of ion concentrations and the identification of their main sources. The results showed that the average pH value of snow in Northwest China was close to 7, and it was slightly higher in Altay than in Heihe. The major cation in snow was Ca^{2+}, and the anion concentration varied greatly. The concentration of ions in the snow in both places decreased in 2019/2020, especially in the Altay region. The average concentration of each ion in snow pits was higher than that in surface snow. The average value of the total concentration of ions in snow in the Altay region was higher than that in the Heihe region.

The temporal variation of the ions in the snowpack was relatively consistent, indicating that the source and migration path of the ions were highly consistent. In the spatial dimension, the ion concentration in the study area was lower than that in industrial developed areas such as Northeast China and Russia but higher than that in other remote areas at high altitude or high latitude.

The results of ion correlation and material source analysis showed that the $EF_{(seawater)}$ values of all ions in the snow were larger than 1, especially Ca^{2+}, indicating that the ions were enriched relative to seawater and mainly came from soil dust. The inputs of Cl^{-} and Na^{+} in snow were mainly from marine sources, but also from terrestrial sources. SO_4^{2-} and NO_3^{-} had stronger correlations than other ions. Therefore, in addition to the input of soil dust, SO_4^{2-} and NO_3^{-} were related to anthropogenic sources.

The back trajectory analysis showed that the study area was mainly affected by local air mass, and the long-distance air mass mainly came from the west. The Ca^{2+}, Na^{+}, Cl^{-}, and SO_4^{2-} concentrations were mainly driven by terrestrial dust input, whereas the Na^{+} and Cl^{-} concentrations were also influenced by marine aerosol contributions. Finally, NO_3^{-} and SO_4^{2-} may originate from densely populated areas in Kazakhstan and industrial areas in the southern part of West Siberia.

Data availability statement

The raw data supporting the conclusion of this article will be made available by the authors, without undue reservation.

Ethics statement

Written informed consent was obtained from the relevant individual(s) for the publication of any potentially identifiable images or data included in this article.

Author contributions

This article represents one result of teamwork. YZ: Data processing, paper writing. NW: Theoretical guidance, article revision, funding. BZ: Data processing. WZ: Chemistry experiment. BS: Article revised.

Funding

This research was funded by the Second Tibetan Plateau Scientific Expedition and Research Program (Grant 2019QZKK020102).

Conflict of interest

The authors declare that the research was conducted in the absence of any commercial or financial relationships that could be construed as a potential conflict of interest.

Publisher's note

References

Avak, S. E., Trachsel, J. C., Edebeli, J., Bruetsch, S., Bartels-Rausch, T., Schneebeli, M., et al. (2019). Melt-induced fractionation of major ions and trace elements in an alpine snowpack. *J. Geophys. Research-Earth Surf.* 124, 1647–1657. doi:10.1029/2019jf005026

Bo, X., Xue, X., Xu, J., Du, X., Zhou, B., and Tang, L. (2019). Aviation's emissions and contribution to the air quality in China. *Atmos. Environ.* 201, 121–131. doi:10.1016/j.atmosenv.2019.01.005

Burgard, D. A., Bishop, G. A., and Stedman, D. H. (2006). Remote sensing of ammonia and sulfur dioxide from on-road light duty vehicles. *Environ. Sci. Technol.* 40, 7018–7022. doi:10.1021/es061161r

Cao, Y.-Z., Wang, S., Zhang, G., Luo, J., and Lu, S. (2009). Chemical characteristics of wet precipitation at an urban site of Guangzhou, South China. *Atmos. Reserarch* 94, 462–469. doi:10.1016/j.atmosres.2009.07.004

Church, T. M., Galloway, J. N., Jickells, T. D., and Knap, A. H. (1982). The chemistry of Western Atlantic precipitation at the mid-Atlantic coast and on Bermuda. *J. Geophys. Res. Oceans* 87, 11013–11018. doi:10.1029/JC087iC13p11013

Cui, X., Ren, J., Qin, X., Du, W., Sun, W., Yu, G., et al. (2011). Climatic and environmental records within a shallow ice core at laohugou glacier No.12,Qilian mountains. *J. Glaciol. Geocryol.* 33, 1251–1258.

Cui, X., Ren, J., Qin, X., Sun, W., Yu, G., Wang, Z., et al. (2014). Chemical characteristics and environmental records of a snow-pit at the glacier No. 12 in the Laohugou valley, qilian mountains. *J. Earth Sci.* 25, 379–385. doi:10.1007/s12583-014-0426-6

Dentener, F. J., Carmichael, G. R., Zhang, Y., Lelieveld, J., and Crutzen, P. J. (1996). Role of mineral aerosol as a reactive surface in the global troposphere. *J. Geophys. Res. Atmos.* 101, 22869–22889. doi:10.1029/96JD01818

Dong, Z., Li, Z., Zhang, M., Wang, F., and Wu, L. (2011). Physico-chemical characteristics and environmental significance of snow deposition on Haxilegen glacier No.51 in Tian Shan, China. *J. Mt. Sci.* 8, 484–494. doi:10.1007/s11629-011-1012-3

Filippa, G., Freppaz, M., Williams, M. W., and Zanini, E. (2010). Major element chemistry in inner alpine snowpacks (Aosta Valley Region, NW Italy). *Cold Regions Sci. Technol.* 64, 158–166. doi:10.1016/j.coldregions.2010.07.005

Fuhrer, K., Neftel, A., Anklin, M., Staffelbach, T., and Legrand, M. (1996). High-resolution ammonium ice core record covering a complete glacial-interglacial cycle. *J. Geophys. Res. Atmos.* 101, 4147–4164. doi:10.1029/95JD02903

Galloway, J. N., Likens, G. E., Keene, W. C., and Miller, J. M. (1982). The composition of precipitation in remote areas of the world. *J. Geophys. Res.* 87, 8771–8786. doi:10.1029/JC087iC11p08771

Gandhi, H. S., and Shelef, M. (1991). Effects of sulphur on noble metal automotive catalysts. *Appl. Catal.* 77, 175–186. doi:10.1016/0166-9834(91)80063-3

Haeberli, W., Schmid, W., and Wagenbach, D. (1988). On the geometry, flow and age of firn and ice at the Colle Gnifetti core drilling site (Monte Rosa, Swiss Alps). *Z. für Gletscherkd. Glazialgeol.* 24, 1–19.

Hall, S. J., Maurer, G., Hoch, S. W., Taylor, R., and Bowling, D. R. (2014). Impacts of anthropogenic emissions and cold air pools on urban to montane gradients of snowpack ion concentrations in the Wasatch Mountains, Utah. *Atmos. Environ.* 98, 231–241. doi:10.1016/j.atmosenv.2014.08.076

He, H.-z., Liu, X.-l., and Zhu, G.-f. (2019). Chemical characteristics and influencing factors of snow in eastern Qilian Mountains, China. *J. Mt. Sci.* 16, 2015–2027. doi:10.1007/s11629-018-5068-1

He, Y. Q., Yao, T. D., Zhang, X. J., Chen, T., Yang, M. X., Sun, W. Z., et al. (2001). Contemporary processes of environmental information in the atmosphere-glacier-runoff system in an area of typical monsoon temperate glacier. *Sci. China Ser. D-Earth Sci.* 44, 275–283. doi:10.1007/bf02911997

Huai, T., Durbin, T. D., Miller, J. W., Pisano, J. T., Sauer, C. G., Rhee, S. H., et al. (2003). Investigation of NH3 emissions from new technology vehicles as a function of vehicle operating conditions. *Environ. Sci. Technol.* 37 (21), 4841–4847. doi:10.1021/es030403+

Jain, M., Kulshrestha, U. C., Sarkar, A. K., and Parashar, D. C. (2000). Influence of crustal aerosols on wet deposition at urban and rural sites in India. *Atmos. Environ.* 34, 5129–5137. doi:10.1016/s1352-2310(00)00350-2

Jeong, D. I., and Sushama, L. (2018). Rain-on-snow events over North America based on two Canadian regional climate models. *Clim. Dyn.* 50, 303–316. doi:10.1007/s00382-017-3609-x

Kang, S. C., Qin, D. H., Mayewski, P. A., Sneed, S. B., and Yao, T. (2002). Chemical composition of fresh snow on Xixabangma peak, central Himalaya, during the summer monsoon season. *J. Glaciol.* 48, 337–339. doi:10.3189/172756502781831467

Kang, S. C., Mayewski, P. A., Qin, D. H., Sneed, S. A., Ren, J. W., and Zhang, D. Q. (2004). Seasonal differences in snow chemistry from the vicinity of Mt. Everest, central Himalayas. *Atmos. Environ.* 38, 2819–2829. doi:10.1016/j.atmosenv.2004.02.043

Kawamura, K., Matsumoto, K., Tachibana, E., and Aoki, K. (2012). Low molecular weight (C-1-C-10) monocarboxylic acids, dissolved organic carbon and major inorganic ions in alpine snow pit sequence from a high mountain site, central Japan. *Atmos. Environ.* 62, 272–280. doi:10.1016/j.atmosenv.2012.08.018

Keene, W. C., Pszenny, A. A. P., Galloway, J. N., and Hawley, M. E. (1986). Sea-salt corrections and interpretation of constituent ratios in marine precipitation. *J. Geophys. Res. Atmos.* 91, 6647–6658. doi:10.1029/jd091id06p06647

Kim, J., and Cho, S. (2003). A numerical simulation of present and future acid deposition in North East Asia using a comprehensive acid deposition model. *Atmos. Environ.* 37, 3375–3383. doi:10.1016/s1352-2310(03)00355-8

Kondrat'ev, I. I., Mukha, D. E., Boldeskul, A. G., Yurchenko, S. G., and Lutsenko, T. N. (2017). Chemical composition of precipitation and snow cover in the primorsky Krai. *Russ. Meteorology Hydrology* 42, 64–70. doi:10.3103/s1068373917010083

Kulshrestha, U. C., Granat, L., Engardt, M., and Rodhe, H. (2005). Review of precipitation monitoring studies in India-a search for regional patterns. *Atmos. Environ.* 39, 7403–7419. doi:10.1016/j.atmosenv.2005.08.035

Kulshrestha, U. C., Kulshrestha, M. J., Sekar, R., Sastry, G. S. R., and Vairamani, M. (2003). Chemical characteristics of rainwater at an urban site of south-central India. *Atmos. Environ.* 37, 3019–3026. doi:10.1016/s1352-2310(03)00266-8

Kumar, B., Singh, S., Gupta, G. P., Lone, F. A., and Kulshrestha, U. C. (2016). Long range transport and wet deposition fluxes of major chemical species in snow at gulmarg in north western Himalayas (India). *Aerosol Air Qual. Res.* 16, 606–617. doi:10.4209/aaqr.2015.01.0056

Kuoppamaki, K., Setala, H., Rantalainen, A.-L., and Kotze, D. J. (2014). Urban snow indicates pollution originating from road traffic. *Environ. Pollut.* 195, 56–63. doi:10.1016/j.envpol.2014.08.019

Li, P., and Mi, D. (1983). Distribution of snow cover in China (1983). *J. Glaciol. Geocryol.* 4, 9–18. (in Chinese).

Li, X. Y., Ding, Y. J., Han, T. D., Kang, S. C., Yu, Z. B., and Jing, Z. F. (2019). Seasonal controls of melt water runoff chemistry and chemical weathering at Urumqi Glacier No.1 in central Asia. *Hydrol. Process.* 33, 3258–3281. doi:10.1002/hyp.13555

Li, Q., Jiang, J., Wang, S., Rumchev, K., Mead-Hunter, R., Morawska, L., et al. (2017). Impacts of household coal and biomass combustion on indoor and ambient air quality in China: Current status and implication. *Sci. Total Environ.* 576, 347–361. doi:10.1016/j.scitotenv.2016.10.080

Li, X., Jiang, F., Wang, S., Turdi, M., and Zhang, Z. (2015a). Spatial distribution and potential sources of trace metals in insoluble particles of snow from Urumqi, China. *Environ. Monit. Assess.* 187, 4144. doi:10.1007/s10661-014-4144-4

Li, X., Li, Z., Ding, Y., Liu, S., Zhao, Z., Luo, L., et al. (2007). Seasonal variations of pH and electrical conductivity in a snow-firn pack on Glacier No. 1, eastern Tianshan, China. *Cold Regions Sci. Technol.* 48, 55–63. doi:10.1016/j.coldregions.2006.09.006

Li, Z., Edwards, R., Mosley-Thompson, E., Wang, F., Dong, Z., You, X., et al. (2005). "Seasonal variability of ionic concentrations in surface snow and elution processes in snow-firn packs at the PGPI site on Urumqi glacier No. 1, eastern Tien Shan, China," in International Symposium on High-Elevation Glaciers and Climate Records, 250. doi:10.3189/172756406781812069

Li, Z. Q., Li, H. L., Dong, Z. W., and Zhang, M. J. (2010). Chemical characteristics and environmental significance of fresh snow deposition on urumqi glacier No. 1 of tianshan mountains, China. *Chin. Geogr. Sci.* 20, 389–397. doi:10.1007/s11769-010-0412-6

Li, Y., Li, J., Liu, Y., and Zhang, P. (2015b). Preliminarily analysis on the characteristics of depth variation of snow accumulation and frozen soil in northern Xinjiang. *Res. Soil Water Conservation* 22, 342–348. (in Chinese).

Li, Z., Edwards, R., Mosley-Thompson, E., Wang, F., Dong, Z., You, X., et al. (2015c). Seasonal variability of ionic concentrations in surface snow and elution processes in snow-firn packs at the PGPI site on Urumqi glacier No.1, eastern Tien Shan, China. *Pap. Present. A. T. Int. Symposium High-Elevation Glaciers Clim. Rec. Lanzhou, PEOPLES R CHINA.*

Li, Z. X., He, Y. Q., Pang, H. X., Yang, X. M., Jia, W. X., Zhang, N. N., et al. (2008). Source of major anions and cations of snowpacks in Hailuogou No.1 glacier, Mt. Gongga and Baishui No.1 glacier, Mt. Yulong. *J. Geogr. Sci.* 18, 115–125. doi:10.1007/s11442-008-0115-4

Li, Z., Li, H., Dong, Z., and Zhang, M. (2010). Chemical characteristics and environmental significance of fresh snow deposition on urumqi glacier No. 1 of tianshan mountains, China. *Chin. Geogr. Sci.* 20, 389–397. doi:10.1007/s11769-010-0412-6

Liu, F., Li, Z., Hao, J., Zhou, X., Wang, F., Zhang, H., et al. (2020). Records of inorganic ions and dust particles in snow at yushugou glacier No. 6 in the desert belt of northwestern China. *Front. Earth Sci.* 8. doi:10.3389/feart.2020.527493

Ma, R., Zhang, M., Wang, S., Wang, J., Yang, S., and Chen, R. (2018). Variation characteristics of snow cover days inWinter in arid region of NorthwestNorthwest China in last 50 years. *J. Nat. Resour.* 33, 127–138. doi:10.11849/zrzyxb.20161261

Macdonald, K. M., Sharma, S., Toom, D., Chivulescu, A., Hanna, S., Bertram, A. K., et al. (2017). Observations of atmospheric chemical deposition to high Arctic snow. *Atmos. Chem. Phys.* 17, 5775–5788. doi:10.5194/acp-17-5775-2017

May, N. W., McNamara, S. M., Wang, S., Kolesar, K. R., Vernon, J., Wolfe, J. P., et al. (2018). Polar plunge: Semester-long snow chemistry research in the general chemistry laboratory. *J. Chem. Educ.* 95, 543–552. doi:10.1021/acs.jchemed.7b00823

Miao, Q., Rosa, R. D., Shi, H., Paredes, P., Zhu, L., Dai, J., et al. (2016). Modeling water use, transpiration and soil evaporation of spring wheat-maize and spring wheat-sunflower relay intercropping using the dual crop coefficient approach. *Agric. Water Manag.* 165, 211–229. doi:10.1016/j.agwat.2015.10.024

Niu, Z., Sun, P., Li, X., He, Y., Huang, C., He, M.-Y., et al. (2020). Spatial characteristics and geographical determinants of mercury and arsenic in snow in northeastern China. *Atmos. Pollut. Res.* 11, 2068–2075. doi:10.1016/j.apr.2020.08.025

Null, S. E., Viers, J. H., and Mount, J. F. (2010). Hydrologic response and watershed sensitivity to climate warming in California's sierra Nevada. *Plos One* 5, e9932. doi:10.1371/journal.pone.0009932

Okada, K., and Kai, K. (2004). Atmospheric mineral particles collected at Qira in the Taklamakan desert, China. *Atmos. Environ.* 38, 6927–6935. doi:10.1016/j.atmosenv.2004.03.078

Okay, C., Akkoyunlu, B. O., and Tayanc, M. (2002). Composition of wet deposition in Kaynarca, Turkey. *Environ. Pollut.* 118, 401–410. doi:10.1016/s0269-7491(01)00292-5

Olivier, S., Blaser, C., Brutsch, S., Frolova, N., Gaggeler, H. W., Henderson, K. A., et al. (2006). Temporal variations of mineral dust, biogenic tracers, and anthropogenic species during the past two centuries from Belukha ice core, Siberian Altai. *J. Geophys. Research-Atmospheres* 111, D05309. doi:10.1029/2005jd005830

Osada, K., Da, H., Kido, M., Matsunaga, K., and Iwasaka, Y. (2004). Mineral dust layers in snow at mount tateyama, central Japan: Formation processes and characteristics. *Tellus Ser. B-Chemical Phys. Meteorology* 56, 382–392. doi:10.1111/j.1600-0889.2004.00108.x

Panicker, A. S., Sandeep, K., Gautam, A. S., Gandhi, N., Beig, G., Nainwal, H. C., et al. (2019). Chemical composition and isotopic signatures of ice and snow over a Himalayan Glacier (Satopanth) in India. *Sn Appl. Sci.* 1, 1166. doi:10.1007/s42452-019-0966-6

Pu, W., Wang, X., Wei, H., Zhou, Y., Shi, J., Hu, Z., et al. (2017). Properties of black carbon and other insoluble light-absorbing particles in seasonal snow of northwestern China. *Cryosphere* 11, 1213–1233. doi:10.5194/tc-11-1213-2017

Qin, D. H., Liu, S. Y., and Li, P. J. (2006). Snow cover distribution, variability, and response to climate change in Western China. *J. Clim.* 19, 1820–1833. doi:10.1175/JCLI3694.1

Rao, Z. G., Wu, D. D., Shi, F. X., Guo, H. C., Cao, J. T., and Chen, F. H. (2019). Reconciling the 'westerlies' and 'monsoon' models: A new hypothesis for the holocene moisture evolution of the xinjiang region, NW China. *Earth-Science Rev.* 191, 263–272. doi:10.1016/j.earscirev.2019.03.002

Sakihama, H., Ishiki, M., and Tokuyama, A. (2008). Chemical characteristics of precipitation in okinawa Island, Japan. *Atmos. Environ.* 42, 2320–2335. doi:10.1016/j.atmosenv.2007.12.026

Singh, S., Gupta, G. P., Kumar, B., and Kulshrestha, U. C. (2014). Comparative study of indoor air pollution using traditional and improved cooking stoves in rural households of Northern India. *Energy Sustain. Dev.* 19, 1–6. doi:10.1016/j.esd.2014.01.007

Steinhauser, G., Sterba, J. H., Foster, M., Grass, F., and Bichler, M. (2008). Heavy metals from pyrotechnics in new years eve snow. *Atmos. Environ.* 42, 8616–8622. doi:10.1016/j.atmosenv.2008.08.023

Sun, Y., Zhuang, G., Huang, K., Li, J., Wang, Q., Wang, Y., et al. (2010). Asian dust over northern China and its impact on the downstream aerosol chemistry in 2004. *J. Geophys. Research-Atmospheres* 115, D00K09. doi:10.1029/2009jd012757

Sundriyal, S., Shukla, T., Tripathee, L., Dobhal, D. P., Tiwari, S. K., and Bhan, U. (2018). Deposition of atmospheric pollutant and their chemical characterization in snow pit profile at Dokriani Glacier, Central Himalaya. *J. Mt. Sci.* 15, 2236–2246. doi:10.1007/s11629-017-4817-x

Taylor, S. R. (1964). Abundance of chemical elements in the continental crust: A new table. *Geochimica Cosmochimica Acta* 28, 1273–1285. doi:10.1016/0016-7037(64)90129-2

Thapa, P., Xu, J., Neupane, B., and Rupakheti, D. (2020). Chemical composition of inorganic and organic species in snow/ice in the glaciers of Western China. *Sci. Total Environ.* 706, 135351. doi:10.1016/j.scitotenv.2019.135351

Thompson, L. G., Yao, T., Mosley-Thompson, E., Davis, M. E., Henderson, K. A., and Lin, P. N. (2000). A high-resolution millennial record of the South Asian Monsoon from Himalayan ice cores. *Science* 289, 1916–1919. doi:10.1126/science.289.5486.1916

Turap, Y., Talifu, D., Wang, X., Abulizi, A., Maihemuti, M., Tursun, Y., et al. (2019). Temporal distribution and source apportionment of PM2.5 chemical composition in Xinjiang, NW-China. *Atmos. Res.* 218, 257–268. doi:10.1016/j.atmosres.2018.12.010

Wake, C. P., Mayewski, P. A., Xie, Z., Wang, P., and Li, Z. (1993). Regional distribution of monsoon and desert dust signals recorded in Asian glaciers. *Geophys. Res. Lett.* 20, 1411–1414. doi:10.1029/93GL01682

Wang, F. T., Li, Z. Q., You, X. N., Li, C. J., Li, H. L., Li, X. Y., et al. (2005). "Seasonal evolution of aerosol stratigraphy in Urumqi glacier No. 1 percolation zone, eastern Tien Shan, China," in International Symposium on High-Elevation Glaciers and Climate Records, 245. doi:10.3189/172756406781812041

Wang, M., Li, Z., Wei, J., Wang, S., Qu, D., and Ying, X. (2016). Major ion characteristics and environmental significance of snow and ice on typical glaciers in qilian mountains. *Res. Environ. Sci.* 29, 1459–1470. doi:10.13198/j.issn.1001-6929.2016.10.09

Wang, P., Yao, T., Tian, L., Wu, G., Li, Z., and Yang, W. (2008). Recent high-resolution glaciochemical record from a Dasuopu firn core of middle Himalayas. *Chin. Sci. Bull.* 53, 418–425. doi:10.1007/s11434-008-0098-7

Wang, X., Pu, W., Zhang, X., Ren, Y., and Huang, J. (2015). Water-soluble ions and trace elements in surface snow and their potential source regions across northeastern China. *Atmos. Environ.* 114, 57–65. doi:10.1016/j.atmosenv.2015.05.012

Wang, Y., Wai, K. M., Gao, J., Liu, X., Wang, T., and Wang, W. (2008). The impacts of anthropogenic emissions on the precipitation chemistry at an elevated site in North-eastern China. *Atmos. Environ.* 42, 2959–2970. doi:10.1016/j.atmosenv.2007.12.051

Wei, T., Kang, S., Dong, Z., Qin, X., Shao, Y., and Rostami, M. (2020). Natural versus anthropogenic sources and seasonal variability of insoluble precipitation residues at Laohugou Glacier in northeastern Tibetan Plateau. *Environ. Pollut.* 261, 114114. doi:10.1016/j.envpol.2020.114114

Williams, M. W., Tonnessen, K. A., Melack, J. M., and Yang, D. (1992). Sources and spatial variation of the chemical composition of snow in the Tien Shan, China. *Ann. Glaciol.* 16, 25–32. doi:10.1017/S0260305500004778

Wu, G., Wei, Q., Sun, C., Gao, J., Pan, L., and Guo, L. (2016). Determination of major and trace elements in snow in Tianjin, China: A three-heating-season survey and assessment. *Air Qual. Atmos. Health* 9, 687–696. doi:10.1007/s11869-015-0375-y

Xiao, C. D., Qin, D. H., Yao, T. D., Ding, Y. J., Liu, S. Y., Zhao, L., et al. (2008). Progress on observation of cryospheric components and climate-related studies in China. *Adv. Atmos. Sci.* 25, 164–180. doi:10.1007/s00376-008-0164-8

Xu, M., Lue, A., Xu, F., and Wang, B. (2008). Seasonal chemical composition variations of wet deposition in Urumchi, Northwestern China. *Atmos. Environ.* 42, 1042–1048. doi:10.1016/j.atmosenv.2007.11.008

Xue, H., Chen, W., Li, M., Liu, B., Li, G., and Han, X. (2020). *Assessment of major ions and trace elements in snow: A case study across northeastern China, 2017-2018. Chemosphere*, 251. doi:10.1016/j.chemosphere.2020.126328

Yang, T., Huang, F., Li, Q., Bai, L., and Li, L. (2017). Spatial-temporal variation of NDVI for growing season and its relationship with winter snowfall in northern Xinjiang. *Remote Sens. Technol. Appl.* 32, 1132–1140. doi:10.11873/j.issn.1004-0323.2017.6.1132

You, X. N., and Dong, Z. W. (2011). Deposition process of dust microparticles from aerosol to snow-firn pack on glacier No. 1 in eastern tianshan mountains, China. *J. Earth Sci.* 22, 460–469. doi:10.1007/s12583-011-0200-y

Yu, H., Yang, W., Wang, X., Yin, B., Zhang, X., Wang, J., et al. (2019). A seriously sand storm mixed air-polluted area in the margin of Tarim Basin: Temporal-spatial distribution and potential sources. *Sci. Total Environ.* 676, 436–446. doi:10.1016/j.scitotenv.2019.04.298

Zhang, M., Wang, S., Wu, F., Yuan, X., and Zhang, Y. (2007). Chemical compositions of wet precipitation and anthropogenic influences at a developing urban site in southeastern China. *Atmos. Res.* 84, 311–322. doi:10.1016/j.atmosres.2006.09.003

Zhang, N. N., He, Y. Q., Theakstone, W. H., and Pang, H. X. (2010). Chemical composition of aerosol and fresh snow and tourism influences at baishui glacier No. 1 from Mt. Yulong, southeastern Tibetan plateau. *J. Earth Sci.* 21, 199–209. doi:10.1007/s12583-010-0018-z

Zhang, N., He, Y., Cao, J., Ho, K., and Shen, Z. (2012). Long-term trends in chemical composition of precipitation at Lijiang, southeast Tibetan Plateau, southwestern China. *Atmos. Res.* 106, 50–60. doi:10.1016/j.atmosres.2011.11.006

Zhang, R., Hegg, D. A., Huang, J., and Fu, Q. (2013). Source attribution of insoluble light-absorbing particles in seasonal snow across northern China. *Atmos. Chem. Phys.* 13, 6091–6099. doi:10.5194/acp-13-6091-2013

Zhang, Y., Lu, C., Zhang, J., Wang, X., and Li, W. (2018). Emission characteristics and individual particle analysis of metals in fine particles emitted from residential coal burning. *China Environ. Sci.* 38, 3273–3279. doi:10.19674/j.cnki.issn1000-6923.2018.0351

Zhang, Y. X., Schauer, J. J., Zhang, Y. H., Zeng, L. M., Wei, Y. J., Liu, Y., et al. (2017). Characteristics of particulate carbon emissions from real-world Chinese coal combustion. *Environ. Sci. Technol.* 51, 5068–5073. doi:10.1021/es7022576

Zhao, Z., Tian, L., Fischer, E., Li, Z., and Jiao, K. (2008). Study of chemical composition of precipitation at an alpine site and a rural site in the Urumqi River Valley, Eastern Tien Shan, China. *Atmos. Environ.* 42, 8934–8942. doi:10.1016/j.atmosenv.2008.08.003

Zheng, W., Yao, T., Xu, B., and Zhao, H. (2008). Ionic chemistry in snowpits from yamzhog yumco basion. *Environ. Sci.* 29, 1488–1494. doi:10.13227/j.hjkx.2008.06.001

Zhou, Y., Wen, H., Liu, J., Pu, W., Chen, Q., and Wang, X. (2019). The optical characteristics and sources of chromophoric dissolved organic matter (CDOM) in seasonal snow of northwestern China. *Cryosphere* 13, 157–175. doi:10.5194/tc-13-157-2019

Zhu, G., Qin, D., Ren, J., Liang, F., and Tong, H. (2018). Assessment of perception and adaptation to climate-related glacier changes in the arid Rivers Basin in northwestern China. *Theor. Appl. Climatol.* 133, 243–252. doi:10.1007/s00704-017-2181-y